Modeling stationary and evolving discontinuities with finite elements

Nicolas Moes, Eric Bechet

MODELING STATIONARY AND EVOLVING DISCONTINUITIES WITH FINITE ELEMENTS

N. Moës and E. Béchet

Ecole Centrale de Nante
1 Rue de la Noë, 44321 Nantes FRANCE
e-mail: nicolas.moes@ec-nantes.fr - Web page: http://www.ec-nantes.fr

Key words: Arbitrary Discontinuity, Fracture, X-FEM, level sets

Abstract. *A methodology for treating non-planar three-dimensional cracks with geometries that are independent of the mesh is summarized. The method is based on the extended finite element method, in which the crack discontinuity is introduced as a Heaviside step function via a partition of unity. In addition, branch functions are introduced for all elements containing the crack front. The crack geometry is described by two signed distance functions (level sets), which in turn can be defined by nodal values. Consequently, no explicit representation of the crack is needed. A Hamilton-Jacobi equation is used to update the level sets as the crack grows. Numerical experiments show the robustness of the method in treating cracks with significant changes in topology. The method is readily extendable to inelastic fracture problems.*

1 Introduction

Three dimensional fracture analysis of engineering problem by standard finite element methods is still quite difficult because of the need to construct a mesh which conforms to both the crack surfaces and the surfaces of the component. If the crack surface is not aligned with the element boundaries, the displacement discontinuity and the traction conditions on the crack surface cannot be treated by standard finite element methods. Furthermore, for standard elements, the mesh must be designed so that it is substantially more refined around the crack than in the remainder of the model. The difficulties are further amplified when considering the growth of cracks, because then the model must be remeshed in the vicinity of the crack. In addition to this, it must be borne in mind that initial cracks in many locations of the component must be considered for a complete engineering analysis.

This paper summarizes a method presented in [1] and [2], in which a three dimensional version of the extended finite element method is developed and applied. The extended finite element method alleviates much of the burden associated with mesh generation for objects with cracks by not requiring the finite elements to conform to the crack surface. Moreover, it provides a convenient way for incorporating near-tip asymptotic fields, so that good accuracy can be obtained for elastic fracture with relatively coarse meshes around the crack.

The essential idea in X-FEM is to use a displacement field approximation that can model an arbitrary discontinuity and the near-tip asymptotic crack fields. As a consequence it is often not necessary to modify the mesh to consider a specific crack; at most, moderate refinement must be introduced around the crack to achieve engineering accuracy in elastic fracture mechanics.

The methodology was first presented in [3, 4, 5]. It was shown that discontinuous functions can be used to enrich finite element approximations via the partition of unity concept introduced by [6]. The resulting approximation can treat cracks that are arbitrarily aligned in the finite element mesh with great accuracy. The concept was generalized in [7] and in [8], which described the application of the concept to arbitrary discontinuities. [9] illustrated the potential of combining the extended finite element method with level sets by solving several problems involving inclusions and holes. In [10], the extended finite element methodology was combined with a level set method to provide a general method for growing cracks. All of the preceding papers dealt with two dimensional problems.

The first application of the extended finite element method to three-dimensional cracks was [11], who solved several planar crack mode I problems and showed that the method compared well with analytical and benchmark solutions. Subsequently [12] coupled the method with the fast marching method to solve several planar crack growth problems in three dimensions.

In this paper, the methodology is extended and modified so that it can handle arbitrary cracks in three dimensions. A key development that facilitates treatment of cracks in three dimensions is the description of crack geometry in terms of two signed distance functions. The displacement field is also described in terms of these signed distance functions. This enables us to construct a near-tip asymptotic field with a discontinuity that conforms to the crack even when it is curved

or kinked near a tip. Furthermore, it eliminates the need for a surface model of the crack. As a consequence, no explicit representation of the crack is needed and the crack is entirely described by nodal data. Although the method will here be described for elastic fracture, it is not limited to linear problems and can easily be extended to nonlinear problems.

We cannot list references to all of the competing methods, but we list some recent papers in the following. The remeshing approach appears to be the most advanced for problems of an industrial type; recent accounts are given by [13] and [14]. Methods which rely on boundary element formulations combined with finite elements are given in [15], [16] and [17]. [18] used the partition of unity concept with the visibility criterion to develop methods for dynamic three dimensional crack growth. Three dimensional dynamic crack growth by the element free Galerkin method has been reported by [19]. The crack surface was represented by a set of triangular elements in 3D, which would be very awkward in a finite element method. The use of finite elements with embedded discontinuities also makes it possible to grow cracks in 2D without remeshing, see [20] and [21] for recent works on the topic.

The methodology for treating arbitrary three dimensional cracks and their evolution by X-FEM are described in this and a companion paper. This paper focuses on the description of cracks in three dimensions in terms of level sets, the computation of the elastic solution and the stress intensity factors (SIFs), whereas the companion paper deals with the update of the level sets needed to model crack growth.

The outline of the paper is as follows. In section 2, the methods for defining the crack geometry and the displacement fields are described. The level sets update scheme is given in Section 3. Section 4 reports the numerical experiments of a lens-shaped crack and a penny-shaped crack under tension.

2 Crack and displacement field description

We consider a body Ω with an outer surface Γ and interior crack surfaces $\Gamma_{\rm cr}$. The crack can be treated as a single surface or as two surfaces: $\Gamma_{\rm cr}^+$ and $\Gamma_{\rm cr}^-$. In the latter case, the initial crack surfaces are considered coincident and the outward normals to the surface of the crack are denoted by $\boldsymbol{n}^+$ and $\boldsymbol{n}^-$, respectively.

[10] described a crack geometry in 2D by two signed distance functions. We also use two signed distance functions to describe a crack in 3D as shown in Fig. 1. Note that the definition of the two level set functions is only needed in a neighborhood of the crack. The signed distance function $\phi(\boldsymbol{x})$ defines the surface of the crack. It is given by

$$\phi(\boldsymbol{x}) = \min_{\overline{\boldsymbol{x}}\in\Gamma_{\rm cr}^{\rm ext}} \|\boldsymbol{x}-\overline{\boldsymbol{x}}\| {\rm sign}\left(\boldsymbol{n}^+\cdot(\overline{\boldsymbol{x}}-\boldsymbol{x})\right) \tag{1}$$

where $\boldsymbol{x}=[x,y,z]$ and ${\rm sign}(\cdot)$ is the sign function ${\rm sign}(x)=+1$ if $x>0$ and -1 if $x<0$. We also need a smooth extension of the crack surface $\Gamma_{\rm cr}$, denoted by $\Gamma_{\rm cr}^{\rm ext}$, which includes the entire crack surface, i.e. $\Gamma_{\rm cr}\subset\Gamma_{\rm cr}^{\rm ext}$. The distance function (1) gives the shortest distance of any point $\boldsymbol{x}$ to the extension of the crack surface $\Gamma_{\rm cr}^{\rm ext}$. This corresponds to the orthogonal projection of $\boldsymbol{x}$ on $\Gamma_{\rm cr}^{\rm ext}$.

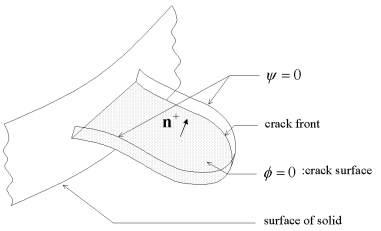

Figure 1: The two iso-zero level sets defining the crack location.

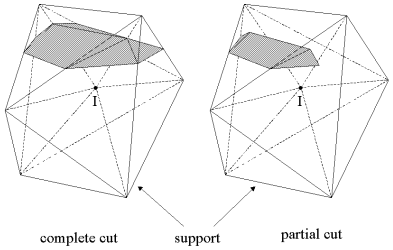

Figure 2: A node I whose support is completely and partially cut by the crack; the support is the volume of the elements connected to node I as shown.

Since the crack surface $\Gamma_{\rm cr}$ is a bounded surface with a crack front, it is also necessary to define the crack front. This is accomplished by using a second signed distance function, $\psi(\boldsymbol{x})$, which is approximately orthogonal to $\phi(\boldsymbol{x})$ so that $\nabla\phi \cdot \nabla\psi \sim 0$. The intersection of the surfaces $\psi(\boldsymbol{x}) = 0$ and $\phi(\boldsymbol{x}) = 0$ gives the crack front; we define the sign of ψ so that $\phi(\boldsymbol{x}) = 0$, $\psi(\boldsymbol{x}) < 0$ gives the crack surface $\Gamma_{\rm cr}$.

The signed distance functions in this paper are approximated by the same shape functions as the displacement field. Therefore, in the computations the signed distance functions are given by

$$\phi = \sum_I N_I(\boldsymbol{x})\phi_I \tag{2}$$

$$\psi = \sum_I N_I(\boldsymbol{x})\psi_I \tag{3}$$

where N_I are the finite element shape functions and ϕ_I and ψ_I are the nodal values of the distance function. This enables the crack shape to be described entirely in terms of nodal values.

The displacement field $\boldsymbol{u}(\boldsymbol{x})$ for the body is decomposed into the continuous and discontinuous parts by

$$\boldsymbol{u} = \boldsymbol{u}_{\rm cont} + \boldsymbol{u}_{\rm dis} \tag{4}$$

where $\boldsymbol{u}_{\rm cont}$ is continuous in Ω, whereas $\boldsymbol{u}_{\rm dis}$ may have several surfaces of discontinuity in Ω. The locations of the discontinuities in $\boldsymbol{u}_{\rm dis}$ are assumed to coincide with $\Gamma_{\rm cr}$.

A standard finite element approximation is used for $\boldsymbol{u}_{\rm cont}$, i.e.

$$\boldsymbol{u}_{\rm cont} = \sum_{I\in\mathcal{N}} N_I(\boldsymbol{x})\boldsymbol{u}_I \tag{5}$$

where $\mathcal{N}$ is the set of all nodes in the mesh, N_I are the classical C^0 shape functions and $\boldsymbol{u}_I$ are displacement nodal degrees of freedom.

For the purpose of constructing the discontinuous field, the nodes are subdivided into three sets :

- $I \in \mathcal{N}_{\text{cut}}$: the set of nodes whose support (union of the elements connected to the node) are completely cut into two, i.e. bisected by the crack surface Γ_{cr}. An example of such a node is shown Figure 2.
- $I \in \mathcal{N}_{\text{branch}}$: the set of nodes whose support are partially cut by the crack surface Γ_{cr}, see Figure 2 for an example of such a node.
- $I \in \mathcal{N} - \mathcal{N}_{\text{cut}} - \mathcal{N}_{\text{cut}}$: the remaining nodes.

The discontinuous displacement fields are given as follows

$$\boldsymbol{u}_{\text{dis}} = \sum_{I \in \mathcal{N}_{\text{cut}}} N_I(\boldsymbol{x}) H(\phi(\boldsymbol{x})) \boldsymbol{a}_I + \sum_{I \in \mathcal{N}_{\text{branch}}} \sum_{\alpha} N_I(\boldsymbol{x}) B_\alpha(\phi(\boldsymbol{x}), \psi(\boldsymbol{x})) \boldsymbol{a}_{I\alpha} \tag{6}$$

In the above, $H(\cdot)$ if the Heaviside step function, $B_\alpha(.,.)$ are branch functions, and $\boldsymbol{a}_I$ and $\boldsymbol{a}_{I\alpha}$ are additional degrees of freedom for the displacement field. The branch functions are constructed in terms of the level sets functions

$$[B_\alpha] = [\sqrt{r}\sin\frac{\theta}{2}, \sqrt{r}\cos\frac{\theta}{2}, \sqrt{r}\sin\frac{\theta}{2}\sin\theta, \sqrt{r}\cos\frac{\theta}{2}\sin\theta] \tag{7}$$

where

$$r = \sqrt{\phi^2 + \psi^2}, \quad \theta = \tan^{-1}(\frac{\phi}{\psi}) \tag{8}$$

Note that the branch functions have been expressed in terms of the level set functions. By expressing the branch functions B_α in terms of the level set functions, it is guaranteed that the discontinuity always corresponds to $\phi = 0$ and $\psi < 0$, i.e. to the surface of the crack. The resulting field will not contain the exact basis of the asymptotic near field, but it is more important to construct the discontinuity in the correct place than to match the exact near-tip asymptotic field.

Only the first of the functions in Eq. (7) is discontinuous across $\phi = 0$. The others were added to improve the accuracy in elastic fracture problems. The above functions span the near-tip asymptotic solution for an elastic crack in two dimensions. In this study and previous studies, see [11], we have also found this basis to be quite accurate for three-dimensional cracks, although we have only considered smooth crack fronts.

This technique of adding asymptotic solutions through the partition of unity in finite elements can be considered an asymptotic matching technique. The displacement fields in the other elements provide the far-field, whereas the elements with the branch functions (7) provide the near field. The finite element procedure then matches these fields so that equilibrium is approximately satisfied.

1- extend V_ψ to the domain

$$\frac{\partial V_\psi}{\partial \tau} + \text{sign}(\psi)\frac{\nabla \psi}{\|\nabla \psi\|} \cdot \nabla V_\psi = 0 \quad \frac{\partial V_\psi}{\partial \tau} + \text{sign}(\phi)\frac{\nabla \phi}{\|\nabla \phi\|} \cdot \nabla V_\psi = 0 \tag{9}$$

2- extend V_ϕ to the domain

$$\frac{\partial V_\phi}{\partial \tau} + \text{sign}(\phi)\frac{\nabla \phi}{\|\nabla \phi\|} \cdot \nabla V_\phi = 0 \quad \frac{\partial V_\phi}{\partial \tau} + \text{sign}(\psi)\frac{\nabla \psi}{\|\nabla \psi\|} \cdot \nabla V_\phi = 0 \tag{10}$$

3- adjustment to prevent modification of previous crack surface

$$\overline{V}_\phi = H(\psi)\frac{V_\phi \psi}{V_\psi \Delta t} \tag{11}$$

4- update and reinitialize the ϕ level set

$$\frac{\partial \phi}{\partial t} + \overline{V}_\phi \|\nabla \phi\| = 0 \quad \frac{\partial \phi}{\partial \tau} + \text{sign}(\phi)(\|\nabla \phi\| - 1) = 0 \tag{12}$$

5- update the ψ level set

$$\frac{\partial \psi}{\partial t} + \overline{V}_\psi \|\nabla \psi\| = 0 \tag{13}$$

6- orthogonalize and reinitialize the ψ level set

$$\frac{\partial \psi}{\partial t} + \text{sign}(\phi)\frac{\nabla \phi}{\|\nabla \phi\|} \cdot \nabla V_\psi = 0 \quad \frac{\partial \psi}{\partial \tau} + \text{sign}(\psi)(\|\nabla \psi\| - 1) = 0 \tag{14}$$

Table 1: Scheme for level set update.

3 Level sets update

The initial level sets representing the crack location are given as data. For many cracks, level set functions which are not signed distance functions can easily be constructed. Then, they may transformed into true signed distance function through a process called initialization, see [2]. The crack velocity on the crack front is given by

$$\boldsymbol{V} = V_\psi \boldsymbol{n}_\psi + V_\phi \boldsymbol{n}_\phi, \quad \boldsymbol{n}_\psi = \frac{\nabla\psi}{\|\nabla\psi\|}, \quad \boldsymbol{n}_\phi = \frac{\nabla\phi}{\|\nabla\phi\|} \tag{15}$$

where $\boldsymbol{n}_\psi$ and $\boldsymbol{n}_\phi$ are the unit normal vectors to the crack front and the crack surface, respectively. The computation of the velocity on the crack front is detailed in the next section. Table 1 summarizes the scheme for the level sets update. In steps 1 and 2, the crack front velocity is extended to all the nodes around the crack front. This extension procedure is classical in the level set method ([22]). The τ indicates a dummy time-like variable whereas the t symbol in the other steps of Table 1 indicates the true time. Equations (9) and (10) are solved in the "τ" time until V_ψ and V_ϕ are stationary, i.e. their derivatives with respect to τ is zero. The steps in Table 1 are explained in more details in [2].

The equations in Table 1 are Hamilton-Jacobi equations of the form

$$\frac{\partial f}{\partial t} + H(\nabla f, \boldsymbol{x}, t) = 0, \quad f(\boldsymbol{x}, 0) = f_0(\boldsymbol{x}) \tag{16}$$

where H is the Hamiltonian. In order to solve these equations they must be discretized in space and time. The level sets are approximated by finite elements:

$$\phi(\boldsymbol{x}, t) = \sum_I N_I(\boldsymbol{x})\phi_I(t), \quad \psi(\boldsymbol{x}, t) = \sum_I N_I(\boldsymbol{x})\psi_I(t) \tag{17}$$

The velocities are approximated by the same shape function:

$$V_\phi(\boldsymbol{x}, t) = \sum_I N_I(\boldsymbol{x})V_{\phi I}(t), \quad V_\psi(\boldsymbol{x}, t) = \sum_I N_I(\boldsymbol{x})V_{\psi I}(t) \tag{18}$$

The level set method has previously been applied to unstructured meshes by [23], and we used the same procedures.

4 Numerical experiment

Two numerical experiments are performed for the growth of a lens-shaped and a penny-shaped crack in a cube under tension. The material properties are elastic and isotropic with Young's modulus $E = 280Gpa$ and Poisson's ratio $\nu = 0.3$. We consider fatigue crack growth governed by the Paris law, which gives the rate of crack growth in mode I in terms of load cycles N by

$$\frac{da}{dN} = CG^m \tag{19}$$

where C is a constant to fit experimental results and G is the maximum energy release rate. We consider the cycles N a time-like variable so the expression for the crack front velocity is

$$\boldsymbol{V} = CG^m(\cos\theta_c \boldsymbol{n}_\psi + \sin\theta_c \boldsymbol{n}_\phi) \tag{20}$$

where θ_c, the angle of the velocity to the plane tangent to the crack (or $\boldsymbol{n}_\phi$), is obtained by

$$\theta_c = 2\text{arctan}\frac{1}{4}\left(\frac{K_I}{K_{II}} - \text{sign}(K_{II})\sqrt{\left(\frac{K_I}{K_{II}}\right)^2 + 8}\right) \tag{21}$$

Thus, the crack growth direction depends on mode I and II stress intensity factors, whereas the crack speed on all three through the energy release rate G. In the numerical study, we chose $m = 1$ and $C = 1$.

As a first example, we consider a cube with a cusp crack subjected to hydrostatic tension as shown in Figure 3. The crack geometry is characterized by the radius R and the azimuthal angle α. A simulation of the evolution of the crack in a cube of $h = 0.01m$ and an initial crack defined by $R = 0.005m$ and $\alpha = 45^o$ is considered. The mesh used is unstructured with 1767 nodes and 8895 tetrahedrons. It is not conforming to the crack and is the same throughout the simulation. From 55 to 67 points were used on the front to compute the crack front velocity and the stress intensity factors. Figure 4 shows the crack after 15 time steps. Note that the initial front has involved into four subfronts in each corner. Furthermore, in this example, one can notice that the convexity of the front has changed : this may be due to the faster growth of the crack near the boundary of the cube.

As a second example, we consider the problem in Figure 5: a cube with an inclined penny-shaped crack subjected to a tensile loading with $h = 0.02m$ and an initial crack defined by $a = b = 0.005m$ and $\alpha = 45^o$. The mesh consists of 1747 nodes and 8847 tetrahedrons. Again, the mesh does not conform to the crack geometry, and the same mesh is used throughout the simulation. Figure 6 shows the evolution of the crack after 17 time steps. From 46 to 58 points were used on the front to compute the stress intensity factors. At the end of the computation, the box is completely cut by the crack. Furthermore, one can notice that the crack front has a complex path. Like the previous problem, at the beginning the front is one entity, then four entities, until the structure is completely cut by the crack.

5 Conclusions

A level set method for arbitrary non-planar cracks in three-dimensional bodies has been presented. The level set technique couples naturally to the extended finite element method, wherein the discontinuous and near-tip asymptotic fields are constructed through a partition of unity. The resulting combined method requires no explicit representation of the crack except in its visualization. Instead, the crack and its growth are described entirely in forms of nodal data. This simplifies the structure of the software and leads to great versatility in treating complex problems in crack growth.

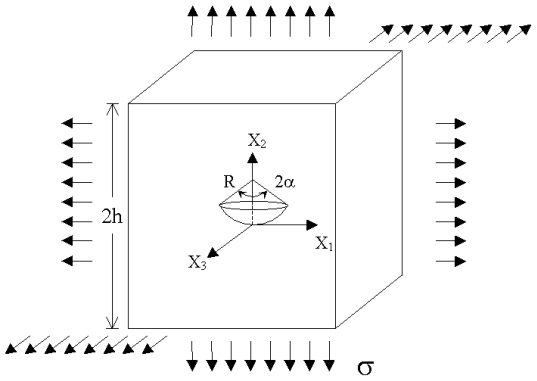

Figure 3: Initial cusp crack subjected to hydrostatic tension.

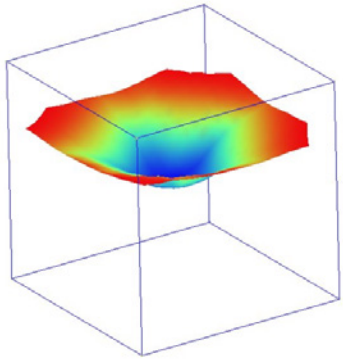

Figure 4: Crack after 15 times steps.

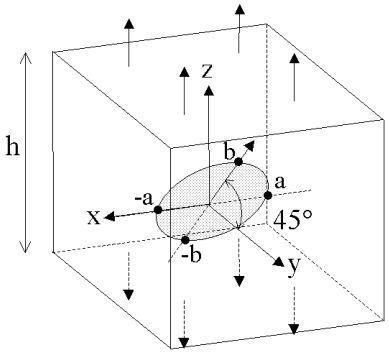

Figure 5: A cube with an inclined penny-shaped crack subjected to a tensile loading.

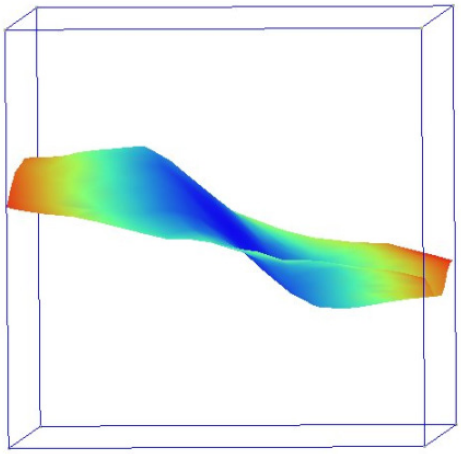

Figure 6: Evolution of the crack after 17 time steps for the inclined penny-shaped crack.

REFERENCES

[1] N. Moës, A. Gravouil, and T. Belytschko. Non-planar 3D crack growth by the extended finite element and level sets. part I: Mechanical model. *International Journal for Numerical Methods in Engineering*, 53:2549–2568, 2002.

[2] A. Gravouil, N. Moës, and T. Belytschko. Non-planar 3d crack growth by the extended finite element and level sets. part II: level set update. *International Journal for Numerical Methods in Engineering*, 53:2569–2586, 2002.

[3] T. Belytschko and T. Black. Elastic crack growth in finite elements with minimal remeshing. *International Journal for Numerical Methods in Engineering*, 45(5):601–620, 1999.

[4] N. Moës, J. Dolbow, and T. Belytschko. A finite element method for crack growth without remeshing. *International Journal for Numerical Methods in Engineering*, 46:131–150, 1999.

[5] J. Dolbow, N. Moës, and T. Belytschko. Discontinuous enrichment in finite elements with a partition of unity method. *Finite elements in analysis and design*, 36:235–260, 2000.

[6] J.M. Melenk and I. Babuška. The partition of unity finite element method: Basic theory and applications. *Comp. Meth. in Applied Mech. and Engrg.*, 39:289–314, 1996.

[7] C. Daux, N. Moës, J. Dolbow, N. Sukumar, and T. Belytschko. Arbitrary branched and intersecting cracks with the eXtended Finite Element Method. *International Journal for Numerical Methods in Engineering*, 48:1741–1760, 2000.

[8] T. Belytschko, N. Moës, S. Usui, and C. Parimi. Arbitrary discontinuities in finite elements. *International Journal for Numerical Methods in Engineering*, 50:993–1013, 2001.

[9] N. Sukumar, D. L. Chopp, N. Moës, and T. Belytschko. Modeling holes and inclusions by level sets in the extended finite element method. *Comp. Meth. in Applied Mech. and Engrg.*, 190:6183–6200, 2001.

[10] M. Stolarska, D. L. Chopp, N. Moës, and T. Belytschko. Modelling crack growth by level sets and the extended finite element method. *International Journal for Numerical Methods in Engineering*, 51(8):943–960, 2001.

[11] N. Sukumar, N. Moës, T. Belytschko, and B. Moran. Extended Finite Element Method for three-dimensional crack modelling. *International Journal for Numerical Methods in Engineering*, 48(11):1549–1570, 2000.

[12] N. Sukumar, D. L. Chopp, and B. Moran. Extended finite element method and fast marching method for three-dimensional fatigue crack propagation. *Engineering Fracture Mechanics*, 2001. submitted.

[13] B.J. Carter, P.A. Wawrzynek, and A.R. Ingraffea. Automated 3d crack growth simulation. *International Journal for Numerical Methods in Engineering*, 47:229–253, 2000.

[14] J.B Cavalcante Neto, P.A. Wawrzynek, M.T.M. Carvalho, L.F. Martha, and A.R. Ingraffea. An algorithm for three-dimensional mesh generation for arbitrary regions with cracks. *Engineering with Computers*, 17(2001):75–91, 2001.

[15] G. Dhondt. automatic 3-d mode i crack propagation calculations with finite elements. *International Journal for Numerical Methods in Engineering*, 41(4):739–757, 1998.

[16] W. H. Gerstle, L. Martha, and A. R. Ingraffea. Finite and boundary element modeling of crack propagation in two- and three-dimensions. *Engineering with Computers*, 2:167–183, 1987.

[17] T. Nishioka and S.N. Atluri. Analytical solution for embedded cracks, and finite element alternating method for elliptical surface cracks, subjected to arbitrary loading. *Engineering Fracture Mechanics*, 17:247–268, 1983.

[18] C. A. Duarte, O. N. Hamzeh, T. J. Liszka, and W. W Tworzydlo. The element partition method for the simulation of three-dimensional dynamic crack propagation. *Comp. Meth. in Applied Mech. and Engrg.*, 2000. in press.

[19] P. Krysl and T. Belytschko. Element free Galerkin method for dynamic propagation of arbitrary 3-d cracks. *International Journal for Numerical Methods in Engineering*, 44(6):767–800, 1999.

[20] G. Bolzon and A. Corigliano. Finite elements with embedded displacement discontinuity: a generalized formulation. *International Journal for Numerical Methods in Engineering*, 549(10):1227–1266, 2001.

[21] T. Jirasek and T. Zimmermann. Embedded crack model: Part I basic formulation. *International Journal for Numerical Methods in Engineering*, 50(6):1269–1290, 2001.

[22] J. A. Sethian. *Level Set Methods & Fast Marching Methods: Evolving Interfaces in Computational Geometry, Fluid Mechanics, Computer Vision, and Materials Science*. Cambridge University Press, Cambridge, UK, 1999.

[23] T. J. Barth and J. A. Sethian. Numerical schemes for the Hamilton-Jacobi and level set equations on triangulated domains. *Journal of Computational Physics*, 145(1):1–40, 1998.